Bragg diffraction in thin 2D refractive index modulated semiconductor samples

Qiong He, Isabelle Zaquine, Gérald Roosen, Robert Frey

Bragg diffraction in thin 2D refractive index modulated semiconductor samples

Qiong He,[1,2] Isabelle Zaquine,[1,*] Gerald Roosen,[2] and Robert Frey[1,2]

[1]*Institut TELECOM/Télécom ParisTech, Laboratoire de Traitement et de Communication de l'Information, CNRS, 46 rue Barrault, 75634 Paris cedex 13, France*

[2]*Laboratoire Charles Fabry de l'Institut d'Optique, Institut d'Optique Graduate School, CNRS et Université Paris Sud, Centre Scientifique Paris Sud, Bât 503, 91403 Orsay cedex, France*

[*]*Corresponding author: isabelle.zaquine@enst.fr*

Received October 17, 2008; accepted December 8, 2008;
posted December 18, 2008 (Doc. ID 102927); published February 4, 2009

A very simple model has been developed to describe the diffractive properties of a crossed grating structure of the refractive index formed by a thin transmission grating recorded in a Bragg reflector. When the Bragg condition of the transmission grating coincides with the band edge of the reflection grating seen as a one-dimensional photonic crystal, the diffraction efficiency and wavelength selectivity of the transmission grating are highly enhanced and a Bragg diffraction regime can be obtained, even in very thin samples. The model can be used to design micrometric very efficient new diffracting devices for optical signal processing. © 2009 Optical Society of America

OCIS codes: 050.1950, 190.2055, 230.1480.

1. INTRODUCTION

Transmission gratings are widely used for optical signal processing [1]. Their performances are nevertheless limited by the small refractive index modulation that can be obtained in usual nonlinear materials. The thickness is also an issue as it must not be too large if an integrated device is wanted, although the diffraction regime associated with thin crystals is a Raman–Nath regime involving multiple diffracted beams. Besides the already well-known simple [2–4] and double resonance [5–9] in a Fabry–Perot cavity, a new approach using slow light at the band edge of a one-dimensional photonic crystal (1D-PC) was recently demonstrated to overcome these difficulties, first in photopolymers [10] and then in semiconductor Bragg reflectors [11]. Results are especially attractive in the latter case due to the high index contrast of Bragg reflectors. The investigations concern the efficiency, wavelength selectivity, and diffraction regime of thin low index modulation transmission gratings when they are recorded in a reflection grating and form a two-dimensional (2D) structure of the refractive index. Huge performance improvements can be obtained when the read beam wavelength and incidence angle correspond to the band-edge resonance of the reflection grating seen as a 1D-PC and satisfy the transmission grating Bragg condition. In this paper, a very simple analytical four-wave model is presented in order to predict the diffraction properties of a 2D refractive index modulated structure and to enable the design of optimized devices for various applications.

The crossed grating device considered in this paper is described in Section 2. The analytical model used to study its diffraction properties is developed in Section 3. Performance enhancement predicted by the model for samples exhibiting a high refractive index step modulation of the reflection grating as seen in semiconductor Bragg mirrors for instance are presented in Section 4 as well as the most favorable case of samples, where the 2D grating is deposited on a mirror that combines the reflected and the transmitted diffracted beams into a single reflected diffracted beam. Finally, the influence of various parameters on the diffractive properties of such samples is detailed.

2. CONSIDERED STRUCTURES AND WAVES

The crossed grating structure has periodicities Λ_x and Λ_z in the x and z directions, respectively (see Fig. 1). The incident beam lies in the xz plane with a small incidence angle θ_R' with respect to the z axis. The grating with fringes parallel to the z direction diffracts in the so-called transmission mode while that recorded with fringes parallel to x operates in the so-called reflection mode [12]. The periodic dielectric permittivity $\varepsilon(z,x)$ satisfies the equation

$$\varepsilon(z + p_z\Lambda_z, x + p_x\Lambda_x) = \varepsilon(z,x), \tag{1}$$

where p_z and p_x are positive or negative integers. For the reflection grating, the Bragg condition (maximum reflection) is satisfied at λ_0 for this incidence angle. However, our aim is not maximum reflection as we wish to maximize the local field [13–17] to enhance the diffraction efficiency of the transmission grating. That is why the 2D periodic structure is designed to operate at the upper band edge of the 1D-PC, herein the reflection grating ($\lambda_{BE} > \lambda_0$), when the read beam incidence angle θ_R' and wavelength λ_{BE} satisfy the transmission grating Bragg condition ($\lambda_{BE} = 2\Lambda_x \sin\theta_R'$). It should be pointed out that the Bragg condition in thick transmission gratings usually ensures maximum diffraction efficiency, whereas here in the case of thin samples, it merely means that the

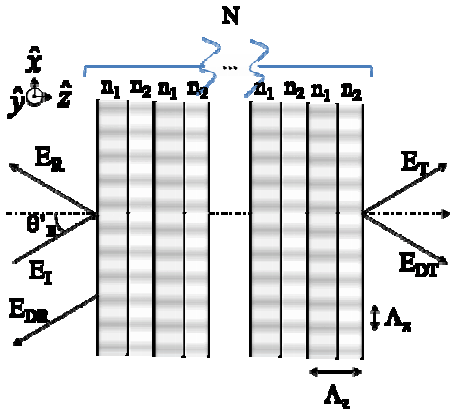

Fig. 1. (Color online) Two-dimensional refractive index modulated structure. In the x direction, the modulation is sinusoidal with a period Λ_x, and in the z direction it is a step modulation made of N pairs of quarter-wave layers of respective indices n_1 and n_2, with a period Λ_z. E_I, E_R, E_T, E_{DT} and E_{DR} are, respectively, the incident, reflected, transmitted, diffracted transmitted, and diffracted reflected waves.

−1 order diffraction angle on the transmission grating is opposite to the incidence angle. In this way, both read and diffracted beams can be enhanced through the band-edge resonance of the reflection grating. This enhancement, giving rise to a single diffracted beam, is possible only if the initial diffraction efficiency of the transmission grating is low. Therefore, we only consider nanostructured materials exhibiting a small refractive index modulation in the x direction. The dielectric permittivity can then be written as

$$\varepsilon(z,x) = \varepsilon(z)[1 + \pi_z(x)], \tag{2}$$

where $\varepsilon(z)$ and $\pi_z(x)$ are periodic in the z and x directions, respectively, $(\varepsilon(z+p_z\Lambda_z)=\varepsilon(z)$ and $\pi_z(x+p_x\Lambda_x)=\pi_z(x)\ll 1)$. Concerning the reflection grating having its wave vector $K_z=2\pi/\Lambda_z$ in the z direction, we are interested in high index modulation step gratings as in multilayered Bragg mirrors. The z dependence of the dielectric permittivity given in Eq. (2) is then

$$\varepsilon(z) = \varepsilon_1 \text{ for } p_z\Lambda_z \leqslant z < p_z\Lambda_z + e_1,$$

$$\varepsilon(z) = \varepsilon_2 \text{ for } p_z\Lambda_z + e_1 \leqslant z < (p_z+1)\Lambda_z, \tag{3}$$

where e_1 is the thickness of the layer of dielectric permittivity ε_1.

For the low modulation refractive index grating along the x direction, $\pi_z(x)$ can then be replaced by the first term of its Fourier expansion (an even function is considered here for the sake of simplicity without any loss of generality)

$$\pi_z(x) = m_{x_1}\cos(K_x x) \text{ for } p_z\Lambda_z \leqslant z < p_z\Lambda_z + e_1,$$

$$\pi_z(x) = m_{x_2}\cos(K_x x) \text{ for } p_z\Lambda_z + e_1 \leqslant z < (p_z+1)\Lambda_z, \tag{4}$$

where $K_x=2\pi/\Lambda_x$ is the wave vector of the transmission grating and m_{xi} $(i=1,2)$ is the permittivity modulation of the transmission grating in the medium of refractive index $n_i=\sqrt{\varepsilon_i}$.

3. MODEL

A. Description

Rather than use a "rigorous coupled waves" method [18–21], where a large number of diffraction orders is taken into account involving large computation times and stability issues, the modeling of this multilayered medium consists of describing the layers separately (Fig. 2). Each dielectric layer is separated from its neighboring layers by two interfaces where reflection takes place because of the dielectric permittivity discontinuity. Moreover, inside each layer, the recorded transmission grating gives rise to diffraction. Our analytical approach of beam propagation (including diffraction on the transmission grating) is based on the nonlinear optics formalism, where only the terms close to phase-matching are kept in the propagation equation. We have then chosen to evaluate how many diffraction orders can reasonably be nonnegligible in the considered structure. As demonstrated hereinafter, the diffraction of an incident read wave $\mathbf{E_I}$ on the crossed gratings structure considered in our study mainly involves four waves in the nonlinear medium (Fig. 2). As the medium with a periodically modulated susceptibility can be considered as infinite in the x axis direction, perfect phase-matching is always achieved in this direction, which determines the direction of the various waves (Fig. 3).

$\mathbf{E_{RFi}}$ is the forward propagating read wave in the medium of refractive index n_i. Only TE polarization has been investigated in this paper but TM polarization would not make much difference considering the small incidence angles used. For the reflection grating with a wave vector $\mathbf{K_z}$ the phase-matching condition gives rise to a single backward propagating diffraction order $\mathbf{E_{RBi}}$ (reflected beam) in which the direction is determined by the Descartes laws at the interfaces between adjacent layers.

Forward and backward diffracted waves $\mathbf{E_{SFi}}$ and $\mathbf{E_{SBi}}$ with wave vectors $\mathbf{k_{SFi}}$ and $\mathbf{k_{SBi}}$ originate from the −1 diffraction order of $\mathbf{E_{RFi}}$ and $\mathbf{E_{RBi}}$ with wave vectors $\mathbf{k_{RFi}}$ and $\mathbf{k_{RBi}}$ on the transmission grating of wave vector $\mathbf{K}_x$,

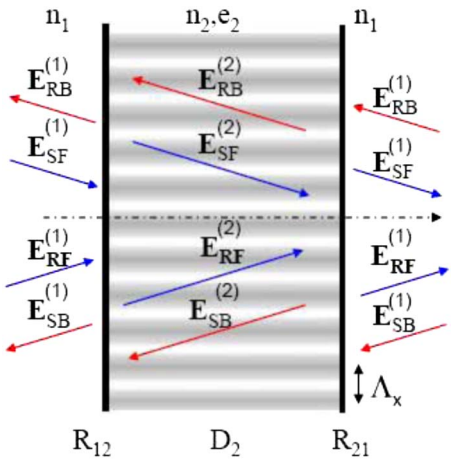

Fig. 2. (Color online) Four main waves taken into account in the crossed gratings structure are shown in one quarter-wave layer with an index n_2 and a thickness $e_2=\Lambda_z-e_1$. Each wave is represented by the direction of its wave vector. The matrix D_2 describes the diffraction in the layer and the matrices R_{12} and R_{21} the reflection at interfaces between layers.

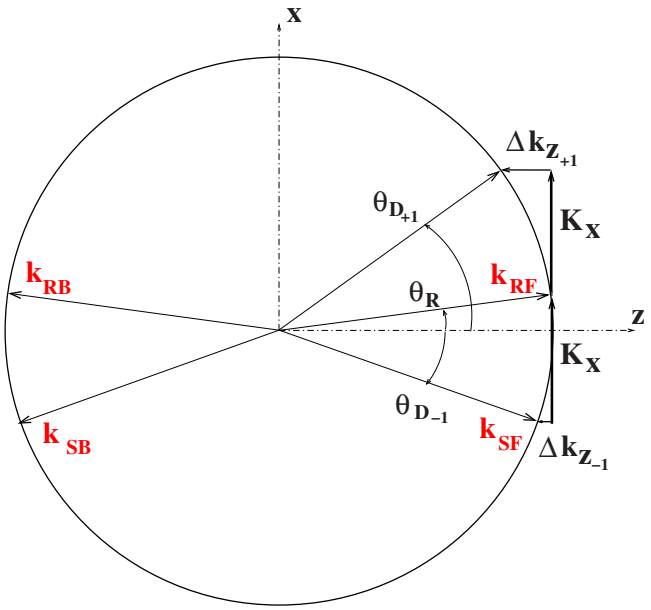

Fig. 3. (Color online) Phase-matching conditions for the four main waves in the photonic crystal when the read beam is not at Bragg incidence. The +1 diffraction order is also represented exhibiting a much larger phase mismatch than the −1 order. The "i" subscript referring to the considered layer type ($i=1,2$) has been omitted.

and the diffraction properties of the device can be accurately described by using only these four waves as will be justified later by computing the intensity of the strongest phase mismatched diffraction order, the +1 order.

If the read wave incidence on the transmission grating with respect to the z axis is θ_{Ri} ($n_i \sin\theta_{\mathrm{Ri}} = \sin\theta'_R$) in the medium with a refractive index n_i, and the read wavelength λ_{BE}, then the direction θ_{D-1i} of the −1 order diffracted wave in the same medium is given by the phase-matching condition in the x direction (Fig. 3)

$$\theta_{D_{-1i}} = \mathrm{Arcsin}[-\lambda_{\mathrm{BE}}/(n_i\Lambda_x) + \sin(\theta_{\mathrm{Ri}})]. \tag{5}$$

At Bragg incidence on the transmission grating ($\sin(\theta_{\mathrm{Ri}}) = \lambda_{\mathrm{BE}}/(2n_i\Lambda_x)$) the symmetry between the read and −1 diffraction order waves ($\theta_{D_{-1i}} = -\theta_{\mathrm{Ri}}$) provides them with the same band-edge enhancement.

The propagation direction of the +1 diffraction order is

$$\theta_{D_{+1}i} = \mathrm{Arcsin}[\lambda_{\mathrm{BE}}/(n_i\Lambda_x) + \sin(\theta_{\mathrm{Ri}})]. \tag{6}$$

Therefore, it does not benefit from the local field enhancement of the 1D-PC band edge. The very simple four-wave model that is detailed hereinafter can be used either to calculate the −1 diffraction order or the +1 diffraction order, provided the right diffraction angles are taken into account. The depletion of the read beam by the −1 diffraction order is not taken into account when computing the +1 order, which leads to an overestimation of the intensity of this higher diffraction order. It will be nevertheless demonstrated that its intensity is very small compared to that of the main diffraction order and that the Bragg diffraction regime can be easily obtained in most situations.

B. Matrix Resolution

In our analysis, the diffraction properties of the 2D device are naturally described using a matrix formalism. A four-dimensional (4D) vector is formed in each layer with the complex amplitudes of the read wave, the reflected wave, the diffracted wave, and the reflected diffracted (or diffracted reflected) wave so that reflection on an interface and diffraction on the transmission grating in one layer can be represented by 4×4 matrices.

At every interface between adjacent layers, the reflection matrix is deduced from the boundary equations [22]

$$\begin{pmatrix} E_{\mathrm{RF}_i} \\ E_{\mathrm{RB}_i} \\ E_{\mathrm{SF}_i} \\ E_{\mathrm{SB}_i} \end{pmatrix} = R_{ij} \begin{pmatrix} E_{\mathrm{RF}_j} \\ E_{\mathrm{RB}_j} \\ E_{\mathrm{SF}_j} \\ E_{\mathrm{SB}_j} \end{pmatrix} = \frac{1}{t_{ij}} \begin{pmatrix} 1 & r_{ij} & 0 & 0 \\ r_{ij} & 1 & 0 & 0 \\ 0 & 0 & 1 & r_{ij} \\ 0 & 0 & r_{ij} & 1 \end{pmatrix} \begin{pmatrix} E_{\mathrm{RF}_j} \\ E_{\mathrm{RB}_j} \\ E_{\mathrm{SF}_j} \\ E_{\mathrm{SB}_j} \end{pmatrix}, \tag{7}$$

where $r_{ij} = (n_i\cos\theta_i - n_j\cos\theta_j)/(n_i\cos\theta_i + n_j\cos\theta_j)$ and $t_{ij} = 2n_i\cos\theta_i/(n_i\cos\theta_i + n_j\cos\theta_j)$; n_i and θ_i are, respectively, the refractive index and propagation angle of the forward propagating wave in the layer number i.

To calculate the diffraction matrix, we use the resolution of the coupled wave equations for the forward read and diffracted waves and for the backward read and diffracted waves:

$$\begin{cases} \dfrac{\partial R_{\mathrm{Fi}}}{\partial z} + \dfrac{k''_i}{\cos\theta_{\mathrm{Ri}}} R_{\mathrm{Fi}} = \dfrac{i\pi\Delta n_i}{\lambda\cos\theta_{\mathrm{Ri}}} S_{\mathrm{Fi}} \\ \dfrac{\partial S_{\mathrm{Fi}}}{\partial z} + \left(\dfrac{k''_i}{\cos\theta_{\mathrm{Ri}}} - i\Delta k_i \right) R_{\mathrm{Fi}} = \dfrac{i\pi\Delta n_i}{\lambda\cos\theta_{\mathrm{Di}}} R_{\mathrm{Fi}} \end{cases} \tag{8a}$$

$$\begin{cases} -\dfrac{\partial R_{\mathrm{Bi}}}{\partial z} + \dfrac{k''_i}{\cos\theta_{\mathrm{Ri}}} R_{\mathrm{Bi}} = \dfrac{i\pi\Delta n_i}{\lambda\cos\theta_R} S_B \\ -\dfrac{\partial S_{\mathrm{Bi}}}{\partial z} + \left(\dfrac{k''_i}{\cos\theta_{\mathrm{Ri}}} - i\Delta k_i \right) S_{\mathrm{Bi}} = \dfrac{i\pi\Delta n_i}{\lambda\cos\theta_{\mathrm{Di}}} R_{\mathrm{Bi}}, \end{cases} \tag{8b}$$

where

$$\begin{cases} E_{\mathrm{RFi,RBi}}(z) = R_{\mathrm{Fi,Bi}}(z)\exp(\pm ik_{\mathrm{RFi,RBi}}\cos\theta_{\mathrm{Ri}} z) \\ E_{\mathrm{SFi,SBi}}(z) = S_{\mathrm{Fi,Bi}}(z)\exp(\pm ik_{\mathrm{SFi,SBi}}\cos\theta_{\mathrm{Di}} z) \end{cases}, \tag{9}$$

where $\Delta n_i = n_i m_x/2$ is the refractive index modulation amplitude in a layer of mean refractive index n_i, $k_i = 2\pi n_i/\lambda$ is the common modulus of all wave vectors at wavelength λ, $\Delta k_i = |\mathbf{k_{SF}}_i - \mathbf{k_{RF}}_i + \mathbf{K_x}|$ is the wave vector mismatch associated to the detuning from Bragg resonance on the transmission grating, and the possible loss has been introduced as the imaginary part $k''_i = 2\pi n''_i/\lambda$ of the wave vector.

These two systems of coupled equations can be expressed in a matrix form

$$\frac{\partial S_i(z)}{\partial z} = A_i S_i(z), \tag{10}$$

where $S_i(z) = [R_{\mathrm{Fi}}(z), R_{\mathrm{Bi}}(z), S_{\mathrm{Fi}}(z), S_{\mathrm{Bi}}(z)]'$ is a column matrix and solved by diagonalizing the matrix A_i, $Q_i = P_i^{-1}A_iP_i$, where P_i is the base change matrix and Q_i is diagonal. The solutions are in the form

$$S_i(z) = P_i C_i X_i(z), \tag{11}$$

where X_i is a 4×4 diagonal matrix $(x_j^{(i)}(z)=\exp(q_j^{(i)}z)$ for $j=1,2,3,4)$, and $C_i=[c_1^{(i)},c_2^{(i)},c_3^{(i)},c_4^{(i)}]'$ is a column matrix of integration constants.

The fields $E_i(z)=[E_{\mathrm{RFi}},E_{\mathrm{RBi}},E_{\mathrm{SFi}},E_{\mathrm{SBi}}]'=M_i(z)S_i(z)$ can then be calculated using the diagonal matrix M_i $(m_1^{(i)}(z)=1/m_2^{(i)}(z)=\exp(ik_{\mathrm{RFi}}\cos\theta_{\mathrm{Ri}}z)$ and $m_3^{(i)}(z)=1/m_4^{(i)}(z)=\exp(ik_{\mathrm{RFi}}\cos\theta_{\mathrm{Di}}z))$. The four integration constants of the matrix C_i are then suppressed so that the field amplitudes of the four involved waves at one boundary of the considered layer i can be related to the field amplitudes at the other boundary in a matrix form:

$$\begin{pmatrix} E_{\mathrm{RFi}}(z=0) \\ E_{\mathrm{RBi}}(z=0) \\ E_{\mathrm{SFi}}(z=0) \\ E_{\mathrm{SBi}}(z=0) \end{pmatrix} = D_i \begin{pmatrix} E_{\mathrm{RFi}}(z=l_i) \\ E_{\mathrm{RBi}}(z=l_i) \\ E_{\mathrm{SFi}}(z=l_i) \\ E_{\mathrm{SBi}}(z=l_i) \end{pmatrix}. \tag{12}$$

The multilayer device can then be modeled by a matrix product,

$$\begin{pmatrix} E_I \\ E_R \\ 0 \\ E_{DR} \end{pmatrix} = R_{01}D_1[R_{12}D_2R_{21}D_1]^{N-1}R_{12}D_2R_{2S}\begin{pmatrix} E_T \\ 0 \\ E_{DT} \\ 0 \end{pmatrix}$$

$$= F\begin{pmatrix} E_T \\ 0 \\ E_{DT} \\ 0 \end{pmatrix}, \tag{13}$$

where each layer pair is modeled by the product $R_{12}D_2R_{21}D_1$ and the input output interfaces matrices have to take into account the indices of the external media, either air or a semiconductor substrate.

Using this matrix product, the reflectivity $|E_R/E_I|^2$, transmission $|E_T/E_I|^2$, and diffraction efficiencies $\rho_T=|E_{\mathrm{DT}}/E_I|^2$ and $\rho_R=|E_{\mathrm{DR}}/E_I|^2$ can be computed. The local value of the field amplitude in the multilayered medium can also be calculated. The first higher order diffraction efficiency can be estimated in the same way and compared to the main diffraction order.

4. RESULTS

To obtain a significant band-edge effect, semiconductor quarter-wave layers as they are used in Bragg reflectors have been considered. GaAlAs/AlAs [23] ($n_1=3.184$ and $n_2=2.912$) gives a permittivity modulation along the z axis $m_z=11\%$, GaAlAs/Alox [24] gives $m_z=82\%$, and the highest permittivity modulation considered here is $m_z=125\%$ with GaAlAs/air.

A. Reflection and Diffraction Spectra

As all structures exhibit the same general behavior, we have picked up as a typical case the GaAlAs/Alox structure with the intermediate value of m_z. Figures 4(a) and 4(b) show the reflectivity and the diffraction spectra of the crossed grating structure. The center wavelength ($\lambda_0=1170$ nm) of the reflection grating has been chosen so that the upper band-edge wavelength is 1.5 μm for telecom applications. The sample is made of 20 layer pairs, and the period of the reflection grating is 274.5 nm. The permittivity modulation of the transmission grating is 3.10^{-3} and its period is 8600 nm. The −1 diffraction order gives rise to a transmitted part and a reflected part, that are almost equal, which reduces the diffraction efficiency by a factor of 2. A sharp maximum can be observed at the band-edge wavelength (diffraction efficiency of 16%); the gain in diffraction efficiency is larger than 470 when compared to the same grating if it was recorded in a homogeneous medium, giving clear evidence of the potentiality of the technique. The full width at half-maximum (FWHM) of this resonance is 1.9 nm, a very high wavelength selectivity for a transmission grating. The +1 diffraction order has also been plotted in Fig. 4(b), and the corresponding efficiency is smaller than the −1 order by a factor of 20, which confirms that the +1 diffraction order does not benefit from the band-edge resonance and that a Bragg diffraction regime can be approached despite the small thickness of the device.

To increase the diffraction efficiency, a 100% reflecting mirror can be added at the back of the sample so that all the diffracted intensity can be concentrated in a single re-

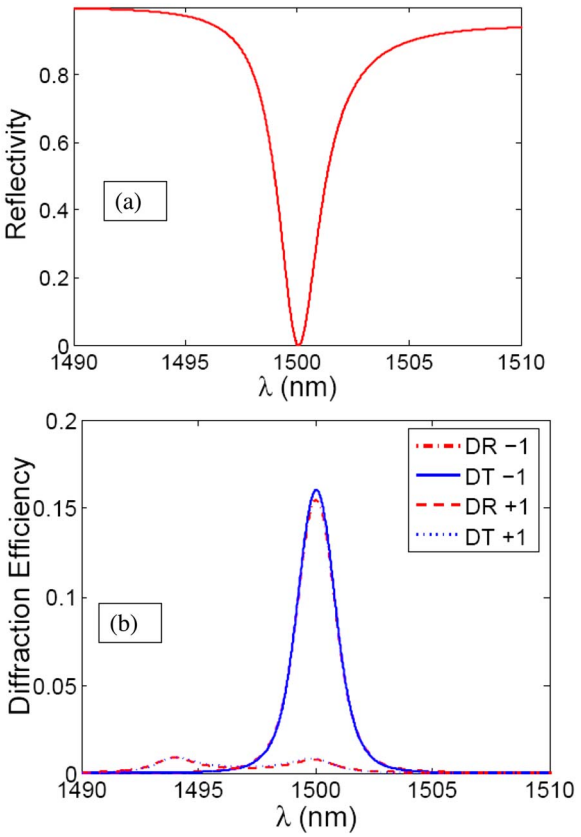

Fig. 4. (Color online) (a) Reflectivity of the 1D-PC. The two semiconductors used are AlGaAs and Alox; there are 20 layer pairs, the thickness is 5.5 μm, the reflection grating period is 274.5 nm, and the band center wavelength is 1.17 μm. (b) Diffraction orders −1 and +1 spectra for the crossed grating device. The two considered diffraction orders give rise to a transmitted beam "DT" and a reflected beam "DR," and the transmission grating period is 8.6 μm; the permittivity modulation along x is 3.10^{-3}.

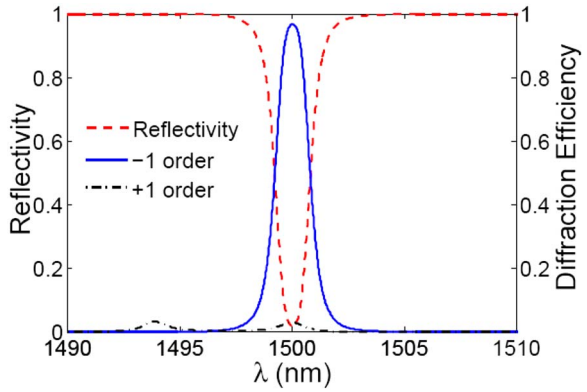

Fig. 5. (Color online) Reflectivity and diffraction efficiency (−1 and +1 diffraction order) of the crossed grating structure with a 100% reflection mirror at the back of the sample. There are 18 layer pairs, the total thickness is 7.6 μm, the reflection grating period is 274.5 nm, and the band center wavelength is 1.17 μm; the transmission grating period is 8.6 μm; the permittivity modulation along x is 3.10^{-3}.

flected diffracted beam. Figure 5 shows that 100% diffraction efficiency can be obtained in that case, even with a thinner crossed grating device (only 18 layer pairs) than in Fig. 4. The FWHM is down to 1.6 nm and the diffraction efficiency ratio of the main order to the higher order is 32, showing that all diffraction properties are improved.

B. Influence of the Structural Parameters

The next step is to calculate the effect of various parameters of the crossed grating structure on the diffractive properties. The maximum diffraction efficiency determines the insertion loss of the device, the width of the resonance at half-maximum (FWHM) gives the wavelength selectivity, and the diffraction efficiency ratio of −1 order to +1 order $R=\rho_{D-1}/\rho_{D+1}$ reflects the diffraction regime of the device. For the transmission grating, index modulation and thickness are the most important parameters. Figure 6 shows the influence of the permittivity modulation m_x for a given thickness $L=14.3$ μm in the case of the AlGaAs/AlAs structure. Diffraction efficiency increases with m_x as expected from Kogelnick's theory for a transmission grating. At the same time, the FWHM also

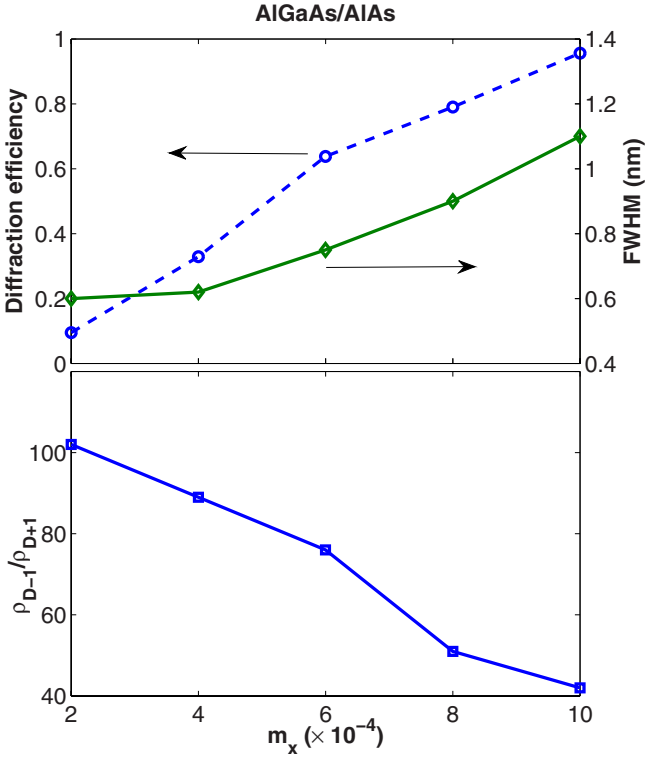

Fig. 6. (Color online) Influence of the permittivity modulation of the transmission grating with a AlGaAs/AlAs reflection grating of 60 layer pairs.

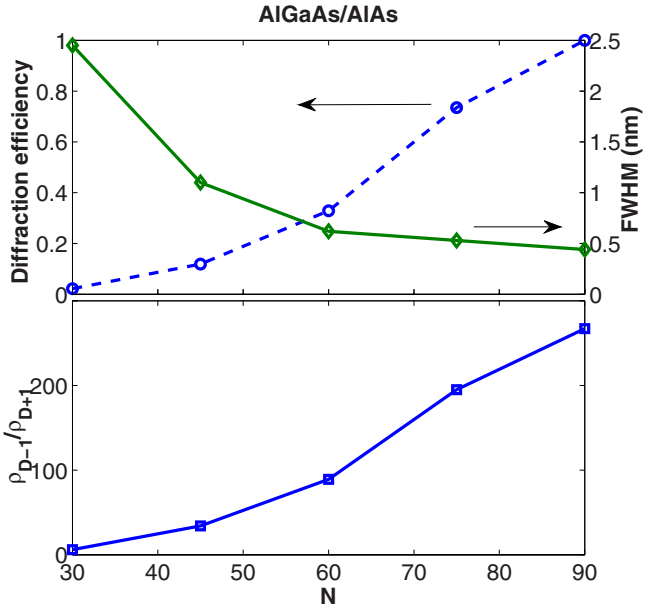

Fig. 7. (Color online) Influence of the number of layer pairs of the AlGaAs/AlAs reflection grating when the permittivity modulation is $m_x=4.10^{-4}$.

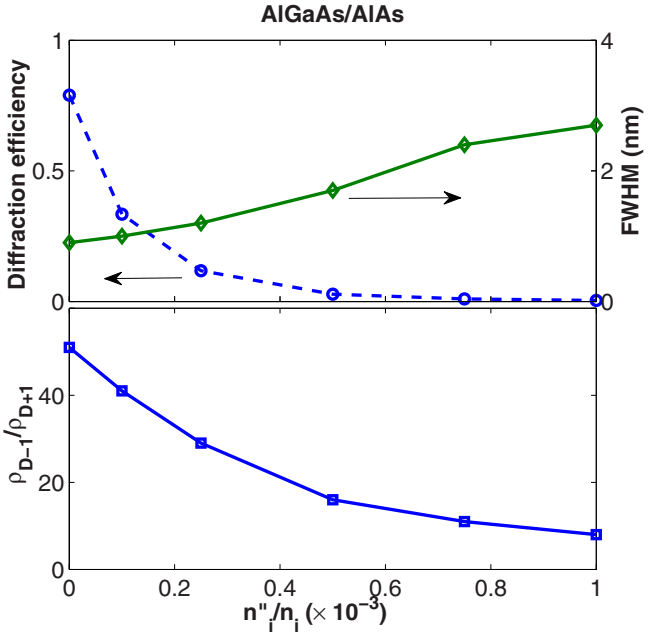

Fig. 8. (Color online) Influence of loss when the permittivity modulation is $m_x=8.10^{-4}$ with a AlGaAs/AlAs reflection grating of 60 layer pairs.

Table 1. Influence of m_z Optimization of the Other Parameters to Obtain Maximum Diffraction Efficiency

Materials	m_z	NN	L (μm)	λ_0 (μm)	m_x ($\times 10^{-3}$)	ρ_{DR-1} (%)	FWHM (nm)	ρ_{DR-1}/ρ_{DR+1}
AlGaAs/AlAs	0.114	60	14.3	1.45	1	95.6	1.1	42
AlGaAs/Alox	0.822	15	4.1	1.166	4.5	95.4	1.4	14
AlGaAs/Alox	0.822	20	5.5	1.171	2	94.2	1.1	66
AlGaAs/Alox	0.822	25	6.9	1.173	1.1	95.3	0.6	215
AlGaAs/air	1.247	10	3.2	0.96	8	95.1	4.3	8
AlGaAs/air	1.247	15	4.8	0.969	2.7	96.8	1.4	65
AlGaAs/air	1.247	20	6.4	0.972	1.1	93.6	0.6	365

increases while the diffraction efficiency ratio of −1 to +1 order decreases when m_x increases, which is not satisfactory for an effective device. This shows that the 2D grating is advantageous only in the case of low index contrast transmission gratings. As predicted by previous works [12], another way to increase diffraction efficiency of a transmission grating is to increase its thickness, and Fig. 7 confirms these results for the crossed gratings structure as the diffraction efficiency, the FWHM, and the diffraction efficiency ratio of orders −1 and +1 are improved when the number of layer pairs N is increased. In this case, all diffractive properties are improved. The 100% diffraction efficiency can be obtained with the thickest sample made of 90 layer pairs if the index modulation along x is 4×10^{-4}. The linewidth is stable beyond 60 layer pairs and does not decrease significantly under 0.5 nm. The same value $N=60$ is also the threshold thickness toward the Bragg diffraction regime as the diffraction efficiency ratio of −1 to +1 order goes over 100. In an actual device, losses must be taken into account even though they may be very low. Figure 8 shows the drastic effect of these losses as they are also enhanced by the band-edge resonance [17]. The diffraction efficiency decreases very steeply and the quasi-Bragg diffraction regime is rapidly lost while the linewidth increases moderately. A very high quality is therefore needed for this device.

C. Influence of the Material

Semiconductor Bragg mirrors can be made of various refractive index contrasts, depending on the chosen materials. For the 2D grating the index modulation along the z axis determines the intensity and the sharpness of the band-edge resonance. Table 1 shows the influence of the permittivity modulation along z. For every value of m_z, the remaining parameters have been chosen in order to obtain a diffraction efficiency close to 100% with a realistic number of layer pairs. When m_z increases this maximum value of the diffraction efficiency can be achieved with less efficient or thinner transmission gratings. In most cases, the diffraction efficiency ratio of −1 to +1 diffraction order is well above the traditional value of 100 considered as the lower limit for a Bragg diffraction regime, which is all the more remarkable as the approximation of the undepleted read beam we have made to calculate the +1 order diffraction efficiency leads to a strong overestimation of this diffraction order when we are close to a 100% diffraction efficiency for the −1 order. These results on higher order intensity validate the very simple four-wave model that has been used for this paper and confirm that a high efficiency diffraction device can be made, even at a micrometric scale.

The optimization could also be made on wavelength selectivity rather than diffraction efficiency criteria with this model, which would of course give different parameters. These calculations show that, using this very simple model, the crossed gratings structure could be easily tailored to a given function as for instance wavelength filtering or beam steering and optimized according to the desired performance. Let us also emphasize that the proposed technology for the implementation of the crossed grating structure is already fully mastered for semiconductor/semiconductor Bragg mirrors. The development of AlGaAs-Alox or semiconductor-air structures deposition techniques is almost complete.

5. CONCLUSION

A simple analytical model has been presented that predicts the diffraction properties of a crossed grating device forming a 2D photonic refractive index modulated structure. Diffraction efficiencies very close to 100% can be obtained as well as high wavelength selectivities and a Bragg diffraction regime, despite the very small thickness of the samples and the low index modulation of the transmission grating, provided optical losses can be minimized. This model can be used for the design of very efficient new micrometric diffracting devices for optical signal processing applications.

REFERENCES

1. E. G. Loewen and E. Popov, *Diffraction Gratings and Applications* (Dekker, 1997).
2. D. D. Nolte, D. H. Olson, G. E. Doran, W. H. Knox, and A. M. Glass "Resonant photodiffractive effect in semi-insulating multiple quantum wells," J. Opt. Soc. Am. B **7**, 2217–2225 (1990).
3. K. M. Kwolek, M. R. Melloch, D. D. Nolte, and G. A. Brost, "Photorefractive asymmetric Fabry–Perot quantum wells: transverse-field geometry," Appl. Phys. Lett. **67**, 736–738 (1995).
4. D. D. Nolte, K. M. Kwolek, C. Lenox, and B. Streetman, "Dynamic holography in a broad-area optically pumped vertical GaAs microcavity," J. Opt. Soc. Am. B **18**, 257–263 (2001).
5. L. Menez, I. Zaquine, A. Maruani, and R. Frey, "Intracavity Bragg gratings," J. Opt. Soc. Am. B **16**, 1849–1855 (1999).
6. L. Menez, I. Zaquine, A. Maruani, and R. Frey, "Experimental investigation of intracavity Bragg gratings," Opt. Lett. **27**, 479–481 (2002).
7. D. Bitauld, I. Zaquine, A. Maruani, and R. Frey,

"Diffraction of Gaussian beams on intracavity Bragg gratings," J. Opt. Soc. Am. B **22**, 1153–1160 (2005).
8. A. Moreau, I. Zaquine, A. Maruani, and R. Frey, "Efficient Bragg-like operation of intracavity low efficiency plane gratings," J. Opt. Soc. Am. B **22**, 2289–2294 (2005).
9. A. Moreau, Q. He, I. Zaquine, A. Maruani, and R. Frey, "Intracavity gain gratings," Opt. Lett. **32**, 208–210 (2007).
10. Q. He, I. Zaquine, A. Maruani, S. Massenot, R. Chevallier, and R. Frey, "Band-edge-induced Bragg diffraction in two-dimensional photonic crystals," Opt. Lett. **31**, 1184–1186 (2006).
11. Q. He, I. Zaquine, A. Maruani, and R. Frey, "Efficient Bragg diffraction in thin semiconductor 2D gratings," Opt. Lett. **33**, 2868–2870 (2008).
12. H. Kogelnik "Coupled wave theory for thick holographic gratings," Bell Syst. Tech. J. **48**, 2909–2947 (1969).
13. R. Frey, Ph. Delaye, and G. Roosen, "Nonlinear optics in nano and microstructures," in *Nanophotonics*, H. Rigneault, J. M. Lourtioz, C. Delalande, and A. Levenson, eds. (ISTE, 2006), p. 187.
14. Ph. Delaye, M. Astic, R. Frey, and G. Roosen, "Transfer-matrix modelling of four-wave mixing at the band-edge of a one-dimensional photonic crystal," J. Opt. Soc. Am. B **22**, 2494–2504 (2005).
15. G. D'Aguanno, M. Centini, C. Sibilia, M. Bertolotti, M. Scalora, M. J. Bloemer, and C. M. Bowden, "Enhancement of $\chi^{(2)}$ cascading processes in one-dimensional photonic bandgap structures," Opt. Lett. **24**, 1663–1665 (1999).
16. Y. Dumeige, P. Vidakovic, S. Sauvage, I. Sagnes, J. A. Levenson, C. Sibilia, M. Centini, G. D'Aquanno, and M. Scalora, "Enhancement of second-harmonic generation in a one-dimensional semiconductor photonic band gap," Appl. Phys. Lett. **78**, 3021–3023 (2001).
17. L. Razzari, D. Trager, M. Astic, Ph. Delaye, R. Frey, G. Roosen, and R. Andre "Kerr and four-wave mixing spectroscopy at the band-edge of one-dimensional photonic crystals," Appl. Phys. Lett. **86**, 231106 (2005).
18. M. G. Moharam and T. K. Gaylord, "Rigorous coupled-wave analysis of planar grating diffraction," J. Opt. Soc. Am. A **71**, 811–818 (1981).
19. M. G. Moharam and T. K. Gaylord, "Three-dimensional vector coupled-wave analysis of planar grating diffraction," J. Opt. Soc. Am. A **73**, 1105–1112 (1983).
20. M. G. Moharam and T. K. Gaylord, "Formulation for stable and efficient implementation of the rigorous coupled-wave analysis of binary gratings," J. Opt. Soc. Am. A **12**, 1068–1076 (1995).
21. M. G. Moharam and T. K. Gaylord, "Rigorous coupled-wave analysis of planar grating diffraction," J. Opt. Soc. Am. A **12**, 1077–1086 (1995).
22. G. Chartier, *Manuel d'Optique* (Hermes, 1997).
23. S. Adachi "GaAs, AlAs and AlGaAs material parameters for use in research and device applications," J. Appl. Phys. **58**, R1–R29 (1985).
24. P.-C. Ku, J. Hernandez, and C. Chang-Hasnain, "Buried selectively oxidized AlGaAs structures on non planar substrates," Opt. Express **10**, 1003–1008 (2002).